

RESEARCH ARTICLE

Mitochondrial plasticity in the cerebellum of two anoxia-tolerant sharks: contrasting responses to anoxia/re-oxygenation

Jules B. L. Devaux^{1,*}, Anthony J. R. Hickey¹ and Gillian M. C. Renshaw²

ABSTRACT

Exposure to anoxia leads to rapid ATP depletion, alters metabolic pathways and exacerbates succinate accumulation. Upon re-oxygenation, the preferential oxidation of accumulated succinate most often impairs mitochondrial function. Few species can survive prolonged periods of hypoxia and anoxia at tropical temperatures and those that do may rely on mitochondria plasticity in response to disruptions to oxygen availability. Two carpet sharks, the epaulette shark (*Hemiscyllium ocellatum*) and the grey carpet shark (*Chiloscyllium punctatum*) display different adaptive responses to prolonged anoxia: while *H. ocellatum* enters energy-conserving metabolic depression, *C. punctatum* temporarily elevates its haematocrit, prolonging oxygen delivery. High-resolution respirometry was used to investigate mitochondrial function in the cerebellum, a highly metabolically active organ that is oxygen sensitive and vulnerable to injury after anoxia/re-oxygenation (AR). Succinate was titrated into cerebellar preparations *in vitro*, with or without pre-exposure to AR, then the activity of mitochondrial complexes was examined. As in most vertebrates, *C. punctatum* mitochondria significantly increased succinate oxidation rates, with impaired complex I function post-AR. In contrast, *H. ocellatum* mitochondria inhibited succinate oxidation rates and both complex I and II capacities were conserved, resulting in preservation of oxidative phosphorylation capacity post-AR. Divergent mitochondrial plasticity elicited by elevated succinate post-AR parallels the inherently divergent physiological adaptations of these animals to prolonged anoxia, namely the absence (*C. punctatum*) and presence (*H. ocellatum*) of metabolic depression. As anoxia tolerance in these species also occurs at temperatures close to that for humans, examining their mitochondrial responses to AR could provide insights for novel interventions in clinical settings.

KEY WORDS: Mitochondria, Anoxia tolerance, Succinate, Brain, Shark, Oxygen

INTRODUCTION

An adequate and continuous supply of oxygen is fundamental to fuelling vertebrate respiration. If the supply of oxygen is severely diminished in mammalian species, survival is limited to a few minutes unless they have adaptations to survive deep-sea diving, hibernation or stress-induced torpor. In the absence of specialised

biochemical and physiological readjustments, hypoxia or anoxia can compromise cellular energy supplies, triggering signal cascades that result in organ failure and subsequently death. Sub-cellularly, anoxia can result in irreversible damage to mitochondria (Andrienko et al., 2017; Javadov, 2015), which can induce the release cytochrome *c*, an initiator of cell death by apoptosis (Kinnally et al., 2011). Furthermore, the majority of cell damage occurs during the re-introduction of normal oxygen levels (Kalogeris et al., 2012). Mitochondrial dysfunction does not always lead to cell death; for example, diminished mitochondrial transmembrane potential can be re-established by 72 h post-stress (Tuan et al., 2008).

In species that evolved their anoxia tolerance at temperatures close to 0°C, the duration of extreme anoxia tolerance can extend to months, because hypothermia slows enzymatic reactions, diffusion and energy-consuming processes, all of which spare energetic resources (Rubinsky, 2003). However, the increase in energy consumption associated with increased metabolic rates in species adapted to higher temperatures (~20–25°C), diminishes the survival time for anoxia-tolerant species to a few days or even hours (Lutz and Nilsson, 1997). On tropical reef platforms, temperatures of up to 35°C have been observed (Potts and Swart, 1984) and remarkably some are inhabited by hypoxia- and anoxia-tolerant reef sharks that have evolved their tolerance in the absence of cold-induced survival mechanisms (Nilsson and Renshaw, 2004). Only a few fish have evolved survival mechanisms that protect them from hypoxia and anoxia in tropical environments, such as: African lakes (Chapman et al., 2002), the Amazon (Richards et al., 2007; Val et al., 2015; Val et al., 1998) and warm coral reef waters (Nilsson and Ostlund-Nilsson, 2004; Renshaw et al., 2002; Routley et al., 2002). As some of these tropical hypoxia- and anoxia-tolerant species can survive several hours of hypoxia at mammalian temperatures in contrast to the a few minutes that humans are able to tolerate, they make useful experimental models in which to examine protective mechanisms.

The epaulette shark (*Hemiscyllium ocellatum*) and its close relative the grey carpet shark (*Chiloscyllium punctatum*) represent ancestral vertebrates and are the only elasmobranch species reported to tolerate prolonged anoxia or hypoxia at tropical temperatures (Chapman and Renshaw, 2009; Wise et al., 1998). The grey carpet shark is distributed in northern Australian waters and is widely distributed in Indo-West Pacific regions (Dudgeon et al., 2016) while the epaulette shark is restricted to northern Australian waters and New Guinea (Bennett et al., 2015; Chapman and Renshaw, 2009; Last, 2009). Both species have been observed on reef flats during the day. While *H. ocellatum* has been observed hunting and feeding on reef flats during nocturnal hypoxic conditions, it has not been confirmed whether *C. punctatum* occupy this niche on nocturnal low tides. However, under experimental conditions, *C. punctatum* can sustain around 1 h of anoxia at 25°C, while *H. ocellatum* routinely survives 2.5 h (Chapman et al., 2011; Renshaw et al., 2002; Routley et al., 2002). *Hemiscyllium ocellatum*

¹School of Biological Sciences, The University of Auckland, Auckland 1142, New Zealand. ²Hypoxia and Ischemia Research Unit, School of Allied Sciences, Griffith University, Gold Coast campus, QLD 4222, Australia.

*Author for correspondence (devauxjules@gmail.com)

 J.B.L.D., 0000-0002-5280-3871; A.J.R.H., 0000-0003-3784-4816; G.M.C.R., 0000-0002-4238-321X

List of abbreviations

$aK_{m,S}$	apparent K_m for succinate
ANT	adenine nucleotide translocase
AR	anoxia/re-oxygenation
cAtr	carboxy-atractyloside
CCCP	carbonyl cyanide <i>m</i> -chlorophyll hydrazine
CI	mitochondrial complex I
CII	mitochondrial complex II (or succinate dehydrogenase, SDH)
Ci_{Ca}	CII catalytic capacity
$CII_{coupled}$	CII capacity coupled to Oxphos
$CII_{uncoupled}$	CII capacity uncoupled from Oxphos
ETS	mitochondrial electron transport system
ETS_{max}	ETS capacity
J_{O_2}	mitochondrial respiration rate
L_{ANT}	leak through adenine nucleotide translocase
$L_{residual}$	residual proton leak
L_{total}	total proton leak
nOCR	net Oxphos control ratio
Oxphos	oxidative phosphorylation
RCR	respiratory control ratio
ROS	reactive oxygen species
SDH	succinate dehydrogenase

is capable of metabolic depression and neuronal hypometabolism in response to diminished oxygen (Mulvey and Renshaw, 2000; Stenslökken et al., 2008) through mediators such as adenosine receptors (Renshaw et al., 2002). Neuronal hypometabolism and temporary blindness may act to diminish the demand for ATP (Mulvey and Renshaw, 2000; Stenslökken et al., 2008). *Hemiscyllium ocellatum* increases the production of NO in response to hypoxia, which could enhance oxygen delivery (as discussed in Nilsson and Renshaw, 2004; Renshaw and Dyson, 1999), and depresses mitochondrial O_2 consumption (Brown, 1995; Cooper and Brown, 2008). In addition, *H. ocellatum* are naturally exposed to cycles of nocturnal hypoxia in their natural environment (Nilsson and Renshaw, 2004), which has been demonstrated to pre-condition this species for longer future exposures to hypoxia with early entry into ventilatory and metabolic depression (Routley et al., 2002).

In contrast, *C. punctatum* maintain their metabolic and ventilation rates, and rapidly increase their haematocrit in response to anoxia, most likely via splenic contractions (Chapman and Renshaw, 2009). It was suggested that the O_2 from stored red blood cells could be released, which would ultimately increase the supply of oxygen to metabolically active organs when the O_2 supply is compromised.

It has been proposed that oxidative damage originates during re-oxygenation from an increase in mitochondria-derived reactive oxygen species (ROS; illustrated in Fig. 6), potentially triggering apoptosis and necrosis (Murphy, 2009). While laboratory-based anoxic stress can be well tolerated by both shark species (Chapman and Renshaw, 2009), there is evidence of re-oxygenation-induced oxidative damage in the *H. ocellatum* (Renshaw et al., 2012) even though *H. ocellatum* produces a lower level of reactive species than other elasmobranchs (Hickey et al., 2012). In mammals, it has been demonstrated that succinate accumulates in highly metabolic ischaemic organs (at least in the brain, heart, liver and kidney) as a result of the ischaemia-induced reversal of succinate dehydrogenase (SDH, i.e. mitochondrial complex II or CII) and the partial inhibition of the malate/aspartate shuttle (Chouchani et al., 2014). Upon reperfusion, succinate is oxidised at elevated rates and this drives excess ROS production by the reversal of electron flow at complex I (CI) (discussed in Andrienko et al., 2017). The succinate-

induced ROS can cause oxidative damage that alters mitochondrial function (Paradies et al., 2002) (illustrated in Fig. 6). These detrimental effects of reperfusion in the presence of excess succinate may be further enhanced at elevated temperatures (De Groot and Rauen, 2007).

Intriguingly, the anoxia-tolerant *H. ocellatum* displayed greater mitochondrial membrane stability after an anoxic event than the hypoxia-sensitive shovelnose ray (*Aptychotrema rostrata*) (Hickey et al., 2012). It was proposed that the high mitochondrial membrane stability observed in *H. ocellatum* would act to maintain oxidative phosphorylation (Oxphos) efficiency and decrease ROS production post-anoxia, which would decrease oxidative damage mediated by re-oxygenation (Hickey et al., 2012). Although *H. ocellatum* heart mitochondria are robust in response to an anoxic challenge, the effect of succinate build-up and ROS production on mitochondrial respiratory complexes and mitochondrial efficiency in other highly metabolic tissues such as the brain has yet to be determined. The cerebellum is one of the most vulnerable regions of the brain to damage from a hypoxic insult (Cervós-Navarro and Diemer, 1991). The loss of the righting reflex, controlled by the cerebellum, is the first sign of physiological shut down and evidence suggests that such cerebellar shut down acts to conserve brain energy charge (Renshaw et al., 2002). In addition, the *H. ocellatum* cerebellum: (i) increases the transcription of pro-survival genes in response to recurrent hypoxic preconditioning (Rytkönen et al., 2012); and (ii) makes protective proteomic readjustments following episodes of either hypoxic or anoxic preconditioning (Dowd et al., 2010). It should be noted that cytochrome oxidase levels are significantly decreased by exposure to diminished oxygen, representing neuronal hypometabolism (Mulvey and Renshaw, 2000), which implies that mitochondria turn down electron transport system (ETS) activity in response to hypoxia. This questions whether cerebellum mitochondria are plastic in their response to diminished oxygen and whether they can subsequently recover.

To test whether mitochondrial plasticity is likely to be involved in the tolerance of the *H. ocellatum* and/or *C. punctatum* brain to anoxia, we investigated the tolerance of mitochondria in whole preparations from the cerebellum of each species to an acute episode of AR with and without elevated succinate levels. More specifically, we compared the mitochondrial respiratory capacity and the mitochondrial plasticity (readjustment of respiratory pathway from CI and CII) in responses to graded levels of exogenous succinate in mitochondria either exposed to AR or maintained with sufficient O_2 (controls). Using high-resolution respirometry, we tested the hypothesis that the cerebellum mitochondria from *H. ocellatum* cerebellum would be more resilient to AR than those from *C. punctatum* and that *H. ocellatum* mitochondria would adjust their respiratory characteristics in response to graded exogenous succinate rather than exhibit high CII succinate oxidation rates during re-oxygenation. This is the first report describing both (i) the normal activity of *H. ocellatum* and *C. punctatum* intact mitochondrial population in the cerebellum; and (ii) their responses to an anoxic challenge followed by re-oxygenation. Both experiments were carried out with graded exogenous succinate.

MATERIALS AND METHODS**Animals and housing**

Six sub-adult *Hemiscyllium ocellatum* (Bonnaterre 1788) with a mean \pm s.e.m. mass of 490 ± 83 g were purchased from Cairns Marine (Cairns, Australia) while seven sub-adult *Chiloscyllium punctatum* J. P. Müller and Henle 1838 with a mean mass of 138 ± 31 g

were provided by Sea World (Main Beach, Gold Coast, Australia). Sharks were held in 300 l tanks containing aerated seawater maintained at 22°C and fed daily with fresh raw shrimps. After a week of acclimation, sharks were starved for 2 days prior to the start of the respirometry experiments. The sharks were measured and weighed post-euthanasia (see below) and the cerebellum was weighed prior to homogenisation.

Cerebellum preparation

Tissue homogenates, which avoided shear stress, were chosen over other methods of preparation (i.e. permeabilised brain or isolated mitochondria) because they (i) retain mitochondrial integrity; (ii) retain all sub-populations of mitochondrial *in situ*; and (iii) conserve potential cellular regulators of mitochondrial function (Kondrashova et al., 2009). However, while including the overall mitochondrial characteristics of different sub-populations contained in the shark cerebellum, any potential differences in mitochondrial density were not assessed. Consequently, the reported difference in respiration rates between the two sharks provides information on the overall mitochondrial capacity within a fixed mass of shark cerebellum, and is not intended to examine differences between mitochondrial units (i.e. adjustments within a mitochondrion).

Sharks were euthanized by the addition of 15 ml of 5% benzocaine, dissolved in ethanol, to 1 l seawater for a final dose of 750 mg benzocaine l⁻¹. After ventilation ceased, the absence of a response to the fin pinch test and the loss of righting reflex indicated that euthanasia was complete; the spinal cord was then sectioned at the cranio-vertebral junction and sharks were rapidly dissected. The cerebellum was rapidly removed and immersed in ice-cold biopsy buffer (in mmol l⁻¹: 2.77 CaK₂EGTA, 7.23 K₂EGTA, 5.77 Na₂ATP, 6.56 MgCl₂·6H₂O, 20 taurine, 15 phosphocreatine disodium salt, 20 imidazole, 0.5 DTT, 50 MES potassium salt and 50 sucrose, pH 7.1 at 30°C) (Hickey et al., 2012). The

cerebellum was then gently blotted to remove excess blood and it was weighed in ~150 mg pieces in 800 µl cold MiR05 respiration medium (containing, in mmol l⁻¹: 0.5 EGTA, 3 MgCl₂·6H₂O, 60 K-lactobionate, 20 taurine, 10 KH₂PO₄, 2.5 Hepes and 700 sucrose, with 1 g l⁻¹ BSA essentially free fatty acid, pH 7.2 at 22°C). A portion of the diced cerebellum was gently homogenised by triturating the small pieces through a 10 ml syringe with decreasing gauge needles (16–25 gauge) and allowed to recover for 1 h in cold MiR05 prior to use in respirometry experiments.

Respirometry experiments

A multiple substrate uncoupler inhibitor protocol (SUIT) was performed to assess the effect of AR on: (i) the total proton leak (L_{total}) and the inducible proton leak through adenine nucleotide translocase (L_{ANT}); (ii) CI-mediated respiration and O₂ flux (J_{O_2}) attributed to Oxphos with and without succinate build-up; (iii) ETS capacity and (iv) CII capacity (Fig. 1). Electron input from either CI or CII can be assessed in SUIT protocols with the sequential reconstitution of TCA cycle pathways by the addition of complex specific substrates. The contribution of each complex to ETS reflects putative mitochondrial plasticity because it represents the readjustment of convergent electron pathways to Oxphos (detailed in Gnaiger, 2014). The addition of succinate and rotenone in the absence of CI substrate mediates oxaloacetate accumulation and further competitively inhibits CII (Harris and Manger, 1969). In this study, the CII contribution to Oxphos was determined by the additive effect of excess succinate to CI-mediated Oxphos (with pyruvate, malate and glutamate) because additive electron flow from CI to the Q-junction converges according to a NADH⁺: succinate ratio of at least 4:1 (Gnaiger, 2014).

Whole homogenates from the cerebellum of either *C. punctatum* or *H. ocellatum* (100 µl corresponding to 10–15 mg tissue) were added to the 2 ml chambers of Oroboros O2ks™ respirometers containing aerated MiR05 media at 20°C (261.92 µmol l⁻¹ O₂ at

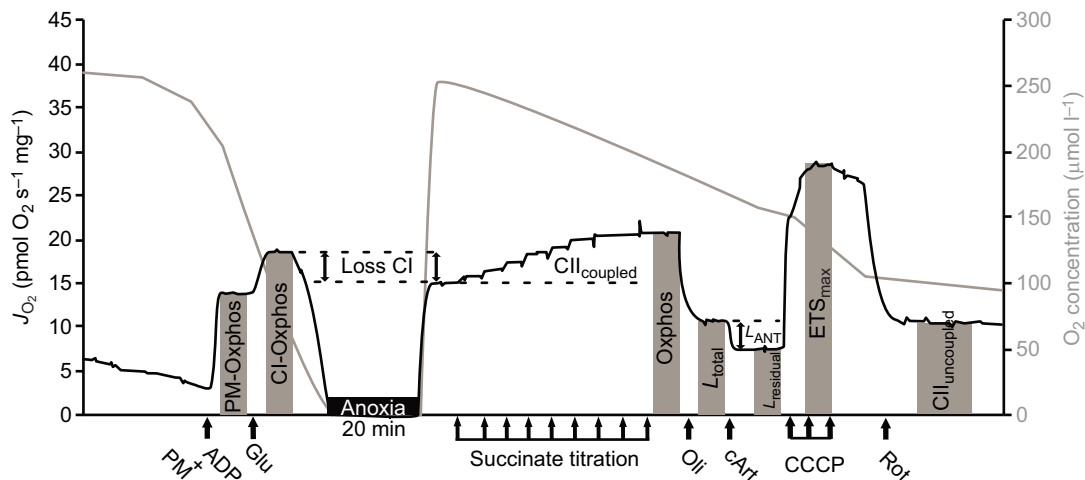


Fig. 1. Representative trace of the substrate uncoupler inhibitor protocol used to measure mitochondrial respiration rates (J_{O_2}) of cerebellum homogenate from grey carpet sharks (*Chiloscyllium punctatum*) and epaulette sharks (*Hemiscyllium ocellatum*). Samples were introduced into the 2 ml respirometer chambers and allowed to recover for 20 min. Excess pyruvate, malate (PM) and ADP were injected to put mitochondria into complex I (CI)-mediated oxidative phosphorylation (PM-Oxphos). The additive effect of glutamate (Glu) was tested by inclusion in the CI substrate addition (CI-Oxphos). The sample was permitted to deplete O₂ until anoxia, and a reference chamber was maintained at between 100 and 250 µmol l⁻¹ O₂ (trace not shown). The chamber was then re-oxygenated after 20 min (up to ~220 µmol l⁻¹ O₂ for both control and anoxic groups). The loss in CI-mediated J_{O_2} (Loss CI) was calculated by anoxia exposure followed by re-oxygenation (AR). Succinate was then titrated up to 10 mmol l⁻¹ to measure the contribution of CII to CI+CII-Oxphos ($J_{CII\ coupled}$). At the conclusion of the experiment, oligomycin (Oli) was added to induce mitochondria in total leak state (L_{total}) and the contribution of the adenine nucleotide translocase (L_{ANT}) was calculated as the difference between L_{total} and the residual leak ($L_{residual}$), which was reached after the addition of the ANT inhibitor carboxy-atractyloside (cAtr). Then, the mitochondria were chemically uncoupled with the titration of CCCP to determine maximum electron transport system capacity (ETS_{max}). Finally, rotenone was added (Rot, a CI inhibitor) to measure the uncoupled CII capacity ($J_{CII\ uncoupled}$).

101.5 kPa barometric pressure). After signal stabilisation, 20 min recovery was sufficient to exhaust routine respiration, and this remaining exhausted respiration was subtracted from the other mitochondrial states. Then, mitochondria CI-linked substrates pyruvate and malate were added at saturated concentrations (10 and 5 mmol l⁻¹, respectively) to assess the non-phosphorylating state mediated by CI input (L_{CI}). Oxidative phosphorylation supported by pyruvate and malate (PM-Oxphos) was then triggered by the addition of 700 $\mu\text{mol l}^{-1}$ ADP and the additional effect of glutamate on mitochondrial respiration was tested by the addition of 10 mmol l⁻¹ glutamate (CI-Oxphos). To test mitochondrial tolerance to AR, mitochondria were allowed to deplete the chamber O₂ then maintained in anoxia for 20 min following re-oxygenation (Hickey et al., 2012); the control group had fully aerated medium.

The amount of tissue in the homogenates (~10–15 mg) was chosen as this permitted anoxic levels to be reached within 30–50 min. After acute anoxic exposure, chambers were exposed to ambient air to re-oxygenate the media up to ~220 $\mu\text{mol l}^{-1}$ O₂ and recommence respiration. Once CI-Oxphos fluxes post-anoxia were determined, a succinate titration (0–10 mmol l⁻¹) was started using an automated titration pump to mimic gradual succinate accumulation. To determine the contribution of AR to altered mitochondrial function, the control tissues were exposed to succinate titration alone in fully aerated medium. Oligomycin was added (5 $\mu\text{mol l}^{-1}$) to determine total leak respiration from combined CI and CII inputs (L_{total}). The fraction of proton leak through the adenine nucleotide translocase (L_{ANT}) was then determined as the difference between L_{total} and the residual leak (L_{residual}), measured by the addition of carboxy-atractyloside (cAtr, 5 $\mu\text{mol l}^{-1}$) to inhibit the ANT. Respiration was then uncoupled from Oxphos using three injections of the protonophore carbonyl cyanide *m*-chlorophenyl hydrazone (CCCP, 0.5 $\mu\text{mol l}^{-1}$ each) to determine the ETS capacity (ETS_{max}). Then, CII capacity uncoupled from Oxphos (CII_{uncoupled}) was assessed by the addition of the CI inhibitor rotenone (0.5 $\mu\text{mol l}^{-1}$), as this represents the maximum capacity of CII to fuel the ETS with electrons, without limitations of the phosphorylating system and without competition for the Q-pool (Gnaiger, 2014). A representative trace of the SUIT protocol and its corresponding effects on mitochondrial respiration are presented in Fig. 1.

Data and statistical analysis

Respirometry fluxes were calculated in real-time with DatLab 6.0 software and expressed in pmol O₂ s⁻¹ mg⁻¹. The data and calculations were transferred to Microsoft Excel (Office v.15.38). The complex I contribution to Oxphos was calculated as the difference between CI-Oxphos and L_{CI} . The CII respiration coupled to Oxphos (CII_{coupled}) was calculated as the difference between Oxphos and CI-Oxphos. The respiratory or acceptor control ratio (RCR) is a function of Oxphos coupling efficiency of a system (Gnaiger, 2014) and was calculated by the formula Oxphos/leak. To estimate how damage to ETS may affect Oxphos, we calculated the net Oxphos control ratio (nOCR) as (Oxphos–leak)/ETS. Dose–response curves for succinate were fitted with the least-squares method using GraphPad Prism 7.0. In addition to the maximum respiration rate derived from the addition of succinate (CII_{coupled}) and the apparent K_m ($aK_{m,S}$; determined as the succinate concentration at which respiration was half of CII_{coupled}), the catalytic efficiency of CII (CII_{cat}; a proxy for enzymatic efficiency, generally represented as V_{max}/K_m) was also presented and calculated as CII_{coupled}/ $aK_{m,S}$.

It should be noted that the use of the term ‘mitochondria’ here does not refer to normalised mitochondrial entities (i.e. if mitochondrial density were established) but denotes all of the mitochondrial populations *in situ* within the cerebellar homogenates. Therefore, mitochondrial characteristics interpreted from respiration rates in the present study yield information about the capacity of mitochondria in the overall tissue, which better indicates the responses that are likely occur in shark cerebellum *in vivo*. It cannot be assumed that all of the results are directly related to mitochondrial adjustments at the organelle level. The data that were used to calculate a number of ratios associated with mitochondrial complexes and leak states did not require quantification of mitochondrial density and the discussion of results is largely based on these ratios.

The Shapiro–Wilk test was used to test for normal distributions. SPSS 23.0 or GraphPad Prism 7.0 were used to perform a Student’s *t*-test when equality of variances was verified. Two-way repeated-measures ANOVA and *post hoc* Tukey’s multiple comparison were performed to compare the effect of substrate–inhibitor on mitochondrial states, to compare the effect of AR on CI contribution, and to compare the additive effect of succinate build-up on mitochondrial respiration rates across species. A significant difference was accepted at $P < 0.05$.

RESULTS

Shark morphology

Sub-adult *C. punctatum* and *H. ocellatum* were used for this study. While *H. ocellatum* had a greater mean body mass than *C. punctatum* (Table 1), the mean proportion of cerebella mass to body mass was greater in *C. punctatum* than in *H. ocellatum*. Neither length nor mass or sex affected mitochondrial function (factorial ANOVA, homogeneity of variance verified with Levene’s test).

Interspecies comparison of cerebellar mitochondrial respiration in fully aerated medium

While the stepwise addition of substrates or inhibitors influenced mitochondrial respiration ($F_{7,42}=153$, $P < 0.001$; Fig. 2), Tukey *post hoc* tests revealed no significant differences in leak states (L_{total} and L_{ANT}) or Oxphos states (CI-Oxphos and Oxphos) between these two closely related carpet shark species. However, *H. ocellatum* homogenates had a significantly higher ETS capacity (ETS_{max}) per mass of tissue than *C. punctatum* mitochondria ($P < 0.001$). The ETS_{max} was ~20% and ~75% higher than Oxphos in *C. punctatum* and *H. ocellatum*, respectively ($P < 0.003$).

Table 1. Morphology of the two anoxia-tolerant sharks

	Body length (cm)	M_b (g)	Cerebellum (mg)/ M_b (g)
Grey carpet shark (6)	53.00±7.57	138.25±30.68	8.58±1.50*
Male (2)	56.00±0.01	121.91±19.74	8.01±0.06
Female (4)	51.00±9.25	143.70±31.72	8.78±1.69
Epauvette shark (6)	67.17±4.15*	490.57±82.91*	1.19±0.13
Male (3)	68.25±0.25	485.57±68.32	1.24±0.14
Female (3)	66.63±4.99	495.57±95.03	1.13±0.10

Body length, body mass (M_b) and the ratio of the cerebellum to M_b for the two anoxia-tolerant shark species, grey carpet shark (*Chiloscyllium punctatum*) and epauvette shark (*Hemiscyllium ocellatum*). The mass of the cerebellum was normalised to body mass for comparison between species. Results are expressed as means±s.e.m. *Significant differences between control and post-anoxia were tested with independent *t*-tests ($P < 0.01$).

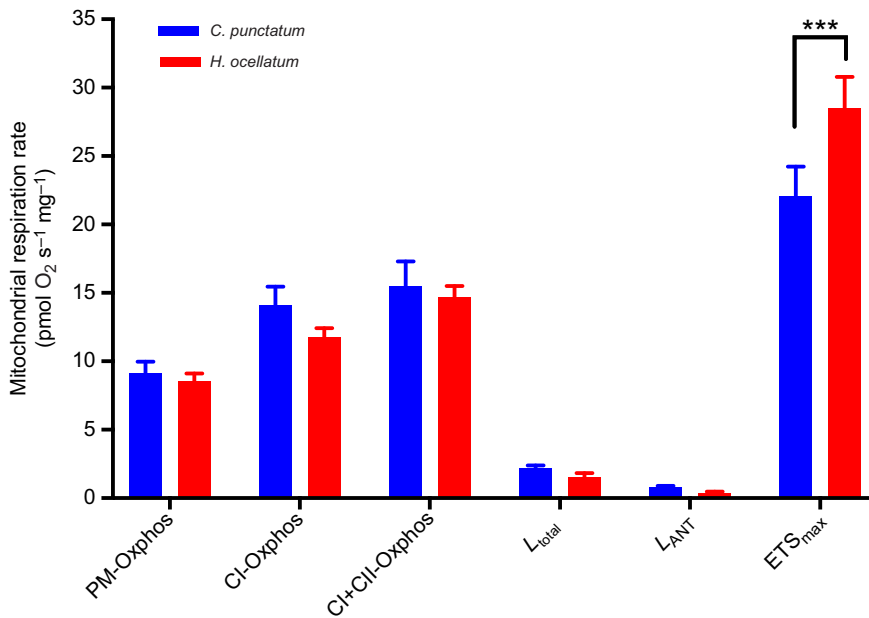


Fig. 2. Mitochondrial respiration rate in homogenates of the cerebellum from two anoxia-tolerant sharks. In PM-Oxphos, there was no difference in respiration rate between *C. punctatum* mitochondria and *H. ocellatum* mitochondria. The addition of excess glutamate to reach CI-Oxphos state followed by excess succinate to reach Oxphos state each mediated an increase of ~ 6 pmol O₂ s⁻¹ mg⁻¹ in both shark species. The addition of oligomycin to measure L_{total} decreased J_{O_2} similarly in the two sharks. L_{ANT} was also similar in the two shark species. However, *H. ocellatum* mitochondria had greater ETS capacity. Refer to Fig. 1 legend for details on the method. Significant differences were tested with two-way ANOVA and *post hoc* test with Tukey correction (***) $P < 0.001$.

Effect of AR on mitochondrial complexes in the two closely related carpet sharks

The overall responses of Oxphos and ETS to AR as well as the contribution of CI and CII to Oxphos were analysed and compared for each species. While Oxphos was significantly decreased by AR in *C. punctatum* homogenates ($P < 0.001$), Oxphos was maintained post-AR in *H. ocellatum* homogenates ($P = 0.15$; Fig. 3). In response to AR, ETS_{max} was significantly decreased in both shark species with a decrease of ~ 31 – 34% ($P < 0.01$) relative to the pre-anoxic state (Table 2).

In mitochondria from *C. punctatum* cerebellum, there was a significant 31% decrease in CI respiration following AR with saturated CI substrates (Fig. 3), which was not compensated for by the 2.7-fold increase in the CII contribution to Oxphos ($P < 0.001$; Fig. 3). We note that this could account for the significant decrease of CI+CII-Oxphos by 26% (corresponding to ~ 4 pmol O₂ s⁻¹ mg⁻¹; $P = 0.04$; Fig. 3). Despite this loss in respiration, RCRs and nOCR were not affected by AR ($P > 0.6$, Table 2). In contrast, CI-mediated respiration was unaffected by AR in mitochondria from *H. ocellatum* cerebella (Table 2 and Fig. 3) and while the level of Oxphos respiration was preserved (Fig. 3), RCRs were significantly decreased, indicating an increase in uncoupled respiration in Oxphos ($P = 0.007$, Table 2). Oxphos capacity was also greater in the *H. ocellatum* cerebellum following AR with a conserved $\sim 91\%$ capacity compared with $\sim 74\%$ in *C. punctatum* mitochondria ($P = 0.05$; Fig. 3).

The contribution of CII to respiration was also tested in two settings (Table 2): coupled to Oxphos (i.e. actual contribution to Oxphos) and uncoupled to Oxphos (full CII capacity to contribute to ETS). In *C. punctatum* homogenates not exposed to AR, CII_{coupled} respiration was ~ 2 pmol O₂ s⁻¹ mg⁻¹ and accounted for only 21% of CII_{uncoupled} ($P < 0.001$). While post-AR the CII_{coupled} increased by $\sim 80\%$ ($P = 0.03$) and matched CII_{uncoupled}, CII overall was diminished by 60% ($P < 0.001$). In contrast, CII_{coupled} reached its full capacity in *H. ocellatum* homogenates not exposed to AR and equated to CII_{uncoupled} (~ 3.5 pmol O₂ s⁻¹ mg⁻¹). Post-AR, however, CII_{coupled} flux was decreased by 35% and equated to 30% CII_{uncoupled} only ($P = 0.02$).

Apparent proton leak

In the normoxic control groups for *H. ocellatum* and *C. punctatum*, L_{total} was similar between species ($P = 0.65$; Figs 2 and 4). However,

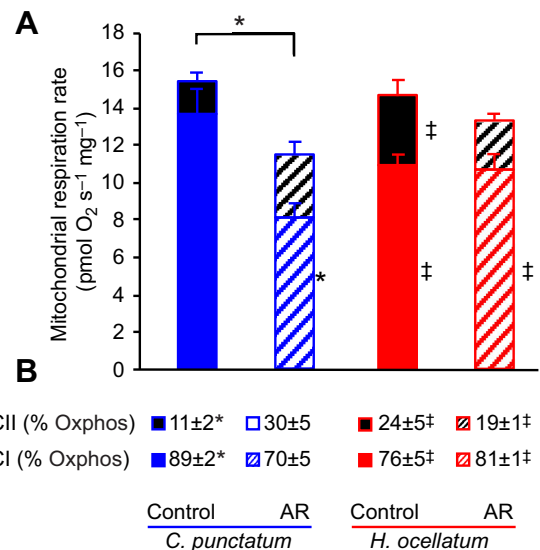


Fig. 3. Contribution of CI and CII to Oxphos before and after exposure to AR. (A) Absolute respiration rates mediated by CI (blue/red) and CII (black) and (B) the relative contributions of each complex to Oxphos in cerebellar homogenates of *C. punctatum* and *H. ocellatum* maintained in normoxia (control, filled) or exposed to an episode of AR (hatched). The CI contribution to respiration was determined in the presence of excess CI-linked substrates (pyruvate, malate and glutamate) followed by ADP while the CII contribution was calculated by the additive effect of succinate on CI-mediated Oxphos respiration rates. Data in A represent the absolute respiration rates mediated by CI and CII, the sum of which corresponds to Oxphos rates, expressed in pmol O₂ s⁻¹ mg⁻¹. Data in B correspond to the relative contribution of each complex to Oxphos rates in tissue exposed to either saturated O₂ or an episode of AR. Results are expressed as means ± s.e.m. ($n = 6$). *Significant difference ($P < 0.05$) between treatments (control and AR); ‡significant difference between shark species (corresponding histograms). The additive effect of the two complexes is shown as stacked histograms, tested with two-way ANOVA with Tukey correction for multiple comparison.

Table 2. Effects of anoxia/re-oxygenation on mitochondrial function in cerebellum homogenates of the two shark species

	CII _{uncoupled} (pmol O ₂ s ⁻¹ mg ⁻¹)	Characteristics of CII _{coupled}			ETS _{max} (pmol O ₂ s ⁻¹ mg ⁻¹)	RCR	nOCR
		aK _{m,S} (mmol l ⁻¹)	CII _{coupled} (pmol O ₂ s ⁻¹ mg ⁻¹)	CII _{cat}			
Grey carpet shark (n=7)							
Control	9.1±0.9 [‡]	0.42±0.18	2.0±0.4 [‡]	4.83	22.0±2.0 [‡]	7.9±1.6	0.59±0.02 [‡]
AR	3.8±0.6* [‡]	1.12±0.30*	3.6±0.7* [‡]	3.23	14.6±0.9* [‡]	7.4±1.3*	0.66±0.03* [‡]
Epauvette shark (n=7)							
Control	3.2±0.5 [‡]	0.90±0.48	4.0±1.1 [‡]	4.47	28.5±2.1 [‡]	9.7±1.1	0.48±0.04 [‡]
AR	5.5±0.6* [‡]	1.37±0.18	2.6±0.3* [‡]	1.69* [‡]	19.8±1.2* [‡]	4.7±0.7*	0.51±0.03 [‡]

The mitochondria in anoxia/re-oxygenation (AR) homogenates and their controls held with sufficient O₂ were uncoupled from Oxphos in the presence of rotenone to determine the CII capacity uncoupled from Oxphos. Three parameters of the CII capacity coupled to Oxphos were extracted using dose–response curves fitted with the least-squares method, and the maximum respiration rate mediated by succinate (CII_{coupled}) and the succinate concentration at which J_{O₂} is half of CII-J_{O₂,max} (aK_{m,S}) were extracted using Prism 7.0. The CII catalytic efficiency (CII_{cat}) was then calculated as CII_{coupled} divided by aK_{m,S}. The respiratory control ratio (RCR) is an estimation of mitochondrial coupling and was calculated using the formula Oxphos/leak. Net oxidative control ration was calculated as (Oxphos–leak)/ETS_{max} and represents the net Oxphos capacity relative to ETS capacity. Results are expressed as means±s.e. *Significant difference between AR and control values; [‡]significant difference between shark species, tested with independent t-tests (P<0.05).

while AR did not affect L_{total} in *C. punctatum* mitochondria, it significantly increased L_{total} by ~58% in *H. ocellatum* mitochondria (P=0.02; Fig. 4). There was no apparent difference in L_{ANT} between the control groups for the two species during pre-AR respiration (Fig. 4). However, following AR, the *H. ocellatum* mitochondria showed a significant ~4-fold increase in L_{ANT} (P=0.035) while L_{ANT} was unchanged in the mitochondria of *C. punctatum*. As L_{residual} was similar in the two species and not affected by AR

(P>0.5), the increase in L_{total} in *H. ocellatum* mitochondria reflected the increase in L_{ANT}.

Effects of titrated exogenous succinate on oxygen flux

Both the succinate concentration and exposure to AR influenced CII-mediated J_{O₂} (F_{3,52}, P=0.015) (Fig. 5). In control groups, the apparent K_m to succinate was similar between the two species (aK_{m,S}≈0.4–0.9 mmol l⁻¹). However, the CII_{coupled} flux was 2-fold higher in *H. ocellatum* cerebellum than in *C. punctatum* cerebellum (P<0.001). In *C. punctatum*, the CII-fuelled respiration was significantly increased post-AR at succinate concentrations above 2 mmol l⁻¹ (P<0.05). A Tukey *post hoc* test revealed that the maximum CII-mediated respiration was significantly increased from 0.5 to 2.5 mmol l⁻¹ succinate in *C. punctatum* (P<0.05). Conversely in *H. ocellatum*, AR mediated a significant decrease in CII-fuelled respiration at succinate concentrations above 0.5 mmol l⁻¹ (P<0.01), and the maximum CII-mediated respiration was decreased at succinate concentrations above 2.5 mmol l⁻¹ (controls) or above 2 mmol l⁻¹ in cerebellar preparations exposed to AR (Fig. 5). Exposure to AR increased aK_{m,S} in *C. punctatum* mitochondria (P<0.001) but not in *H. ocellatum* mitochondria, in which aK_{m,S} was unchanged (Table 2). While aK_{m,S} was doubled in both species after exposure to AR, the capacity of CII to oxidise succinate (CII_{cat}) was maintained in *C. punctatum* compared with their controls, while CII_{cat} was significantly decreased by ~35% relative to control groups in *H. ocellatum* (P<0.001; Table 2).

DISCUSSION

Ultimately, surviving hypoxia or anoxia depends on an animal's ability to conserve energy stores by limiting their ATP demands and/or their ability to produce sufficient ATP despite O₂ limitations and the arrest of Oxphos (Boutilier, 2001). Notably, *H. ocellatum* had a smaller cerebellum relative to their body mass than did *C. punctatum* (Table 1). The metabolic scaling theory based on the relationship between body mass and metabolic rate (reviewed in Agutter and Wheatley, 2004) would support the notion that the cerebellum of *H. ocellatum* may have lower demands for ATP and therefore require less O₂ to sustain cerebellar function than the cerebellum of *C. punctatum*. In addition, *H. ocellatum* has the ability to undergo metabolic depression with clear evidence of neuronal hypometabolism (Mulvey and Renshaw, 2000; Stenslökken et al., 2008), which most likely enables *H. ocellatum* to withstand a longer exposure to limited environmental O₂. Although both species of carpet shark are known to survive

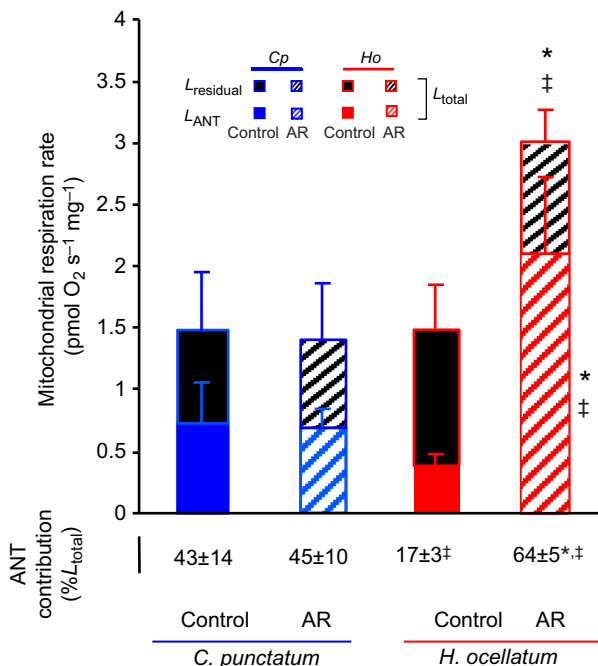


Fig. 4. Mitochondrial respiration attributed to proton leak and the contribution of ANT. Two components of proton leak were measured in cerebellar homogenates from *C. punctatum* (Cp, blue) and *H. ocellatum* (Ho, red) that were exposed to either normoxia (control) or AR. Oligomycin was added to put phosphorylating mitochondria into the leak state (L_{total}). The portion of proton leak through ANT (L_{ANT}) was calculated as the difference between L_{total} and the residual leak (L_{residual}), reached after the addition of carboxy-atractyloside. Both rates are expressed as pmol O₂ s⁻¹ mg⁻¹ with the relative contribution of L_{ANT} to L_{total} (values below main graph). Results are presented as means±s.e.m. (n=6). *Significant difference (P<0.05) between groups (control and AR); [‡]significant difference between species, tested with independent t-tests.

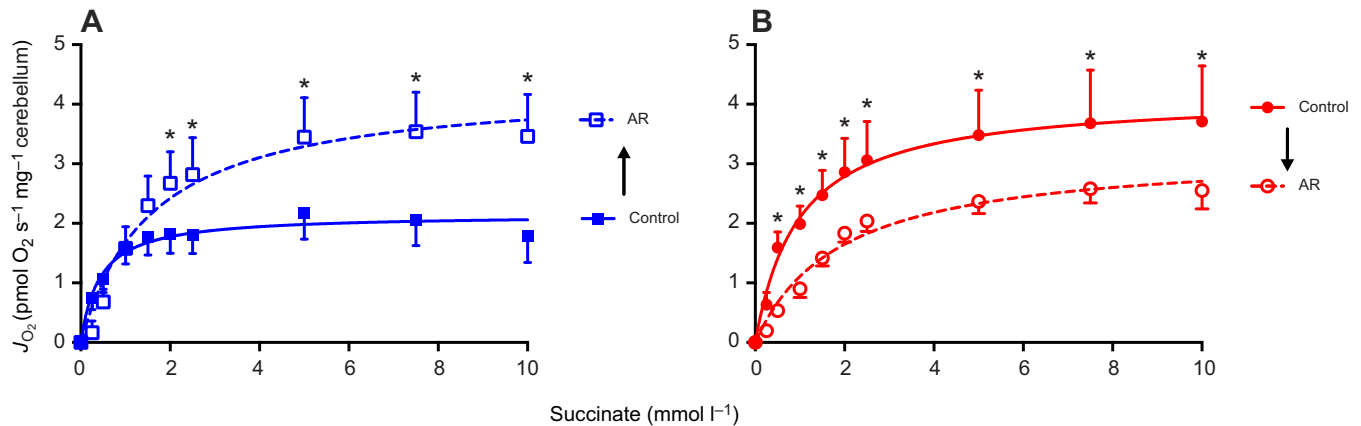


Fig. 5. Comparison of CII respiration rates mediated by increased succinate levels. Data are for mitochondria in normoxia (control, solid lines) or exposed to AR (dashed lines) in the cerebellum of (A) *C. punctatum* or (B) *H. ocellatum*. Mitochondrial respiration in cerebella homogenates from *C. punctatum* (blue) and *H. ocellatum* (red) was measured and dose–response fitted curves extracted as described in Materials and Methods. While AR mediated an increase in CII respiration in mitochondria from *C. punctatum*, CII respiration was decreased in mitochondria of *H. ocellatum*. Results are expressed as means \pm s.e.m. ($n=6$). The effects of succinate increments and AR were tested with a two-way ANOVA repeated-measures test. *Significant difference ($P<0.05$) between groups (control and AR).

prolonged anoxia, the sharks displayed contrasting physiological responses to AR (Chapman and Renshaw, 2009). The *ex vivo* data collected in this study revealed that the contrasting mitochondrial plasticity of these two species of anoxia-tolerant sharks parallels their *in vivo* physiological responses to anoxia: (i) the mitochondria from *H. ocellatum*, which is capable of metabolic depression, decreased metabolism of succinate in response to AR; whereas (ii) the mitochondria from *C. punctatum*, which does not enter metabolic depression, not only continued to use succinate but also increased the rate of succinate metabolism in response to AR.

Mitochondrial integrity with regard to AR

The cerebellum of the two carpet sharks displayed similar mitochondrial characteristics before exposure to AR *in vitro* (Fig. 2). While the data were not corrected for any differences in mitochondrial density, this finding implies that the cerebellum from the two species had the same ability to produce ATP after AR. Both sharks had relatively high (reserve) ETS capacity (i.e. ETS > Oxphos), indicating that the cerebellum of both sharks can accommodate some damage to their ETS without a detrimental effect on Oxphos and ATP production rates. ETS damage may occur during re-oxygenation because in the presence of O₂, electron leakage enhances ROS production and damage to lipids within biological membranes and this compromises ETS (Murphy, 2016; Musatov and Robinson, 2012; Paradies et al., 2002). We note that the *H. ocellatum* cerebellum had a 20% greater ETS capacity than the *C. punctatum* cerebellum, which is likely to confer a substantial advantage against ROS damage in response to AR, because of the maintenance of high coupling and low leak state.

While AR decreased ETS by \sim 30% in both shark species, only the Oxphos rate in *C. punctatum* cerebellum was affected, with a 26% decrease. Previous work using permeabilised *H. ocellatum* heart ventricle fibres showed a \sim 20–60% loss of ETS capacity relative to Oxphos following an anoxic exposure, with minimal change in Oxphos (Hickey et al., 2012) indicating a consistent response to anoxia in *H. ocellatum* mitochondrial populations across cerebellum and heart tissues. Surprisingly, *C. punctatum* homogenate respiration was more tightly coupled to Oxphos (greater RCR) than *H. ocellatum* homogenate respiration. Furthermore, the net Oxphos ratio suggests similar ATP production efficiencies (i.e. similar nOCR) between the sharks.

Overall, while Oxphos rates were lowered in both species, respiration in *C. punctatum* was better coupled to Oxphos and hence more efficiently directed to ATP production. In contrast, respiration was less coupled to Oxphos in *H. ocellatum* cerebellum but Oxphos rates were maintained post-AR. Taken together, these data demonstrate that, in both sharks, cerebella mitochondria exposed to AR appeared to experience ETS damage; however, ATP production rates may remain preserved with a contrasting response between shark species.

Leak and contribution of the ANT

Proton leak results from protons dissipating passively or actively across the inner mitochondrial membrane without passing through the ATP_{F₀-F₁} synthase, and therefore mediates a loss in coupling efficiency of mitochondria (Divakaruni and Brand, 2011). L_{total} (mediated with oligomycin) was similar for the two species and represents around 10% of Oxphos rates, which corresponds to levels previously measured in *H. ocellatum* heart mitochondria (Hickey et al., 2012). Although anoxia followed by re-oxygenation did not affect total proton leak in the *C. punctatum* cerebellum, AR significantly increased the total proton leak in *H. ocellatum* cerebellum to 18% of Oxphos rates.

While counterintuitive, we note that increased proton leak can be beneficial, as it probably prevents elevated ROS production under reduced states (Ali et al., 2012; Rolfe and Brand, 1997), such as with elevated succinate with anoxia (Chouchani et al., 2014). Up to a third of total proton leakage occurs through the ANT (Azzu et al., 2008; Brand et al., 2005). The portion of L_{total} attributed to the ANT increased from 43% pre-anoxia to 63% after AR in the *H. ocellatum*. Similar increases have been observed in rodents displaying enhanced leak through the mitochondrial transition pore (and at least in part through the ANT) after repeated AR episodes (Navet et al., 2006).

Proton leak through the ANT may reflect ADP–ATP exchange rates (Chinopoulos et al., 2014). This increase may therefore favour ADP–ATP exchange between mitochondria and the cytosol and restore cytosolic ATP and mitochondria ADP content (Klingenberg, 2008). Overexpression of the ANT, via the activation of cell-protective pathways (ERK and AKT), has been shown to protect mammalian cardiomyocytes exposed to hypoxia (Winter et al., 2016) or oxidative stress (Klumpe et al., 2016). While the specific

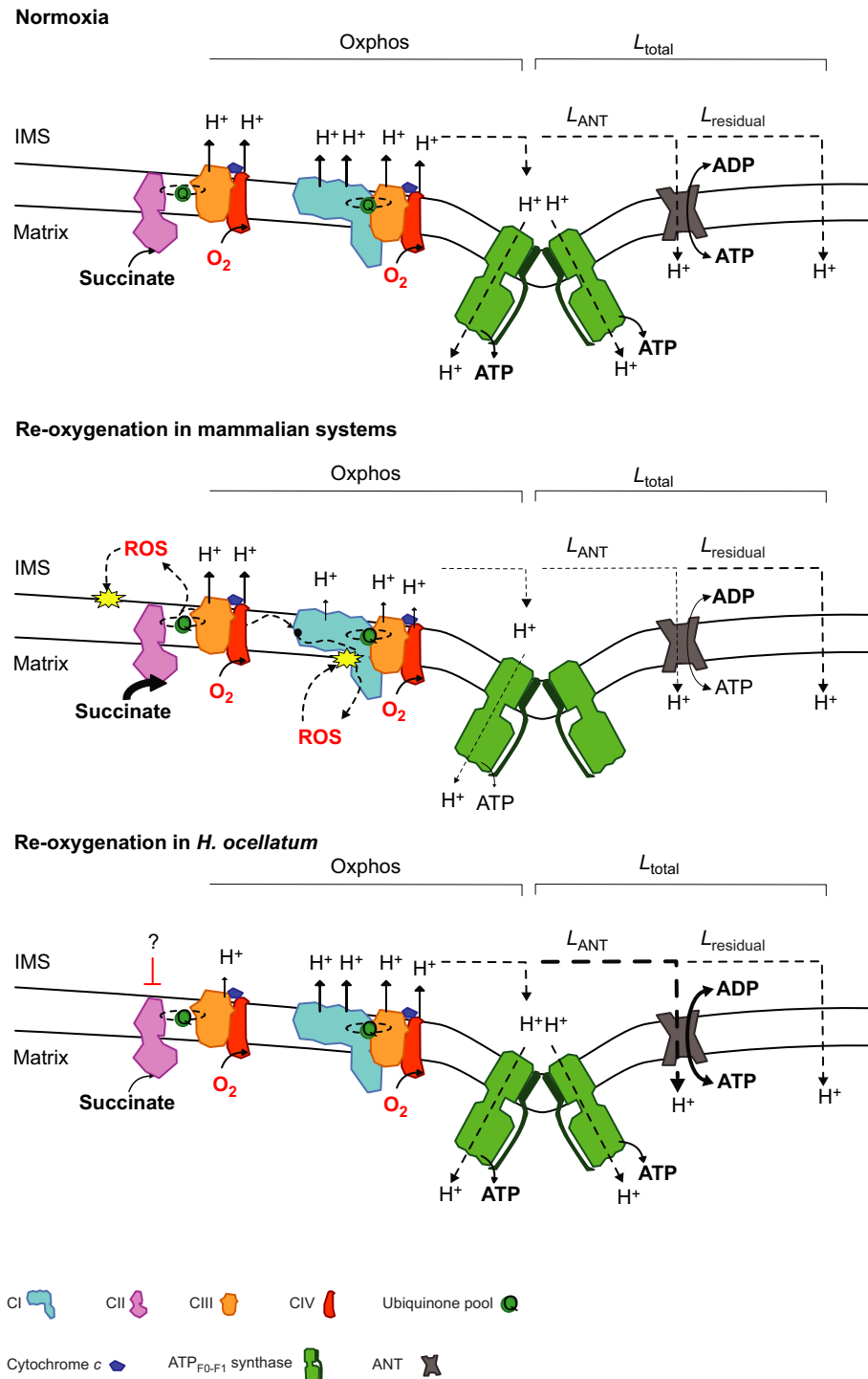


Fig. 6. Oxygen, proton and adenine nucleotide fluxes in the mitochondrial ETS. In normoxic conditions, proton pumping is mediated through CI- and CII-linked systems and the consumption of O₂. The gradient of protons, more concentrated in the inter-membrane space (IMS), is utilised by the ATP_{F0-F1} synthase via Oxphos to produce ATP. Some protons may leak through the membrane or transmembrane proteins, one of which is ANT, which mediates the ADP and ATP exchange between the matrix and the IMS. The proton leak through ANT (L_{ANT}) and other proton leakage ($L_{residual}$) uncouple respiration from Oxphos and this results in the loss of capacity to produce ATP for a given rate of respiration. After an episode of anoxia, succinate accumulates and upon re-oxygenation, succinate oxidation rate accelerates, which mediates an enhanced ROS production from CII, but also a 'reverse electron flow' to CI (Chouchani et al., 2014). This probably affects CI stability and results in an overall loss of capacity for proton pumping and Oxphos. In contrast with the mitochondria of most vertebrates, mitochondria from the epaulette shark (*H. ocellatum*) cerebellum somehow decreases succinate oxidation rate post-AR and CI-linked system capacity is maintained. L_{ANT} was also increased post-AR and this results in the maintenance of Oxphos. The results obtained from this study suggest that the response of *C. punctatum* mitochondria sits between the re-oxygenation and the *H. ocellatum* panels. While succinate oxidation rates were increased post-AR and CI-linked system capacity was decreased, *C. punctatum* maintained Oxphos rates similar to those of *H. ocellatum*, with a greater utilisation of O₂ for Oxphos (lower L_{ANT} and similar $L_{residual}$ relative to *H. ocellatum*).

mechanisms of ANT regulation in *H. ocellatum* mitochondria were not assessed in this study, elevated leak should decrease reverse electron flow, decrease localised O₂ concentration and therefore prevent increased ROS production (Brookes, 2005), possibly temporarily increasing ATP–ADP exchange (Fig. 6).

Mitochondrial plasticity and complex contribution following AR

The capacity of CI and CII to feed the ETS with electrons is essential for Oxphos. CI has been shown to be sensitive to anoxia (Chen et al., 2007; Giusti et al., 2008; Paradies et al., 2004; Rouslin, 1983)

and the most sensitive mitochondrial complex to ROS damage (Hardy et al., 1990; McLennan and Degli Esposti, 2000; Paradies et al., 2004). In this study, CI contribution was tested prior to and after 20 min of anoxia. While the contribution of CI to Oxphos was similar for the two species in normoxia, in the *C. punctatum* mitochondria the CI capacity decreased by ~30% following AR (Fig. 3). The loss of CI J_{O_2} capacity was not fully compensated for by CII and resulted in an overall 26% loss in Oxphos capacity in the *C. punctatum* mitochondria. However, the *H. ocellatum* mitochondria, which appeared to have a greater ETS reserve capacity, also retained proportionately more CI-supported flux

following AR, despite a suppression in CII flux. Hence, O₂ utilisation in *H. ocellatum* mitochondria is more efficiently transferred to proton pumping, which is essential for Oxphos.

In general, enhanced CII activity has been proposed to lead to a greater electron leakage from CII post-anoxia (Quinlan et al., 2012; Tretter et al., 2016; Zakharchenko et al., 2013), which may impact CI capacity through ROS-mediated oxidation of cardiolipin (Paradies et al., 2002). In hypoxia-tolerant *Drosophila*, the suppression of CII activity decreased ROS production and was proposed to improve long-term survival in hypoxia (Ali et al., 2012). Hence, the data on CII suppression in *H. ocellatum* following AR could have a role in preventing damage to CI upon re-oxygenation (Fig. 6). In contrast, within the *C. punctatum* cerebellum, CII was more sensitive to AR, yet provided a greater contribution to respiration than CI.

Succinate accumulation

In normoxic conditions, succinate is better utilised by the *H. ocellatum* mitochondria with a greater CII contribution to Oxphos than *C. punctatum* mitochondria (Fig. 3). Following anoxia, succinate is oxidised more rapidly by *C. punctatum* mitochondria with increased apparent CII catalytic efficiencies. At high concentration (i.e. above 2 mmol l⁻¹), which approximates concentrations in ischaemic mammalian brain (Benzi et al., 1979, 1982; Folbergrová et al., 1974), succinate also mediated higher O₂ flux in *C. punctatum* (Fig. 4). As enhanced succinate oxidation rates on re-oxygenation can trigger reverse electron flow to CI, which impairs the mitochondrial function in murine models (Chouchani et al., 2014; Starkov, 2008), this may explain why CI capacity was decreased post-AR in *C. punctatum*.

In contrast, the overall mitochondrial succinate oxidation rates in the *H. ocellatum* cerebellum were lowered in response to AR even with incremented succinate concentrations and this may suppress ROS production in the *H. ocellatum* cerebellum (Fig. 6). Greater CII catalytic efficiency at low succinate concentrations also suggests that succinate is better utilised by the *H. ocellatum* cerebellum than by the *C. punctatum* cerebellum, which may prevent its accumulation. The downregulation of succinate dehydrogenase activity also occurs within *H. ocellatum* rectal glands after hypoxic exposure (Dowd et al., 2010), and lowered succinate dehydrogenase has been shown to be protective against ischaemia–reperfusion injuries in other animal models (Ali et al., 2012; Pflieger et al., 2015; Wojtovich and Brookes, 2008). Succinate oxidation is also depressed in hibernating squirrels, which experience reperfusion-like injury on arousal (Brown et al., 2012, 2013). While this is as yet unknown, whereas succinate accumulates in the cerebellum of the sharks, inhibition of succinate oxidation may reflect the metabolic suppression observed in *H. ocellatum* (Chapman et al., 2011; Renshaw and Dyson, 1999; Renshaw et al., 2002); furthermore, it may account for the preconditioning effect initiated by a first anoxic exposure which remodelled responses to subsequent insults on a cellular level (Dowd et al., 2010; Rytönen et al., 2012).

Conclusion

Contrasting responses of the *C. punctatum* and *H. ocellatum* cerebella to AR with and without elevated succinate levels highlight key attributes of mitochondrial plasticity used by two tropical anoxia-tolerant species. Despite damage reflected by the decrease in ETS capacity post-AR in both species, Oxphos rates were not changed in the *H. ocellatum* mitochondria and were only marginally lower in *C. punctatum* mitochondria. In this respect, brain mitochondria in these two species are comparatively more robust

than heart mitochondria from the anoxia-sensitive shovelnose ray (Hickey et al., 2012).

Chiloscyllium punctatum mitochondria were surprisingly more efficient in directing O₂ flux to Oxphos, which could result in a greater capacity to produce ATP post-AR. A contrasting strategy which would maintain ATP levels post-AR was observed in *H. ocellatum* mitochondria, which had higher active proton leak rates associated with higher ADP/ATP exchange rates. Such a strategy would help to rapidly restore cytosolic energy stores post-AR.

The data revealed that CI was more robust to AR in *H. ocellatum* cerebellum than in *C. punctatum* cerebellum and that the partial inhibition of CII in *H. ocellatum* may represent the initiation of metabolic depression. Furthermore, CII inhibition in *H. ocellatum* would probably prevent reverse electron flow to CI. Such inhibition is likely to not only preserve CI integrity but also limit ROS production during AR.

This study provides insights into the mitochondrial physiology and plasticity in the brains of two anoxia-tolerant tropical species which can tolerate hypoxia at temperatures close to those of mammals. An understanding of how mitochondrial plasticity occurs in tropical anoxia-tolerant species could lead to novel therapeutic strategies to prevent ischaemia–reperfusion injury in the mammalian brain.

Acknowledgements

The authors would like to thank Dr Oliva Holland, Dr Lan-feng Dong and Professor Jiri Neuzil for graciously providing access to additional OROBOROS™ O₂ks. We also thank Sea World (Gold Coast Australia) for supplying animals and the Smart Water Research Centre for their assistance with housing animals.

Competing interests

The authors declare no competing or financial interests.

Author contributions

Conceptualization: J.B.L.D., A.J.R.H., G.M.C.R.; Methodology: J.B.L.D., A.J.R.H., G.M.C.R.; Software: J.B.L.D., G.M.C.R.; Validation: J.B.L.D., A.J.R.H.; Formal analysis: J.B.L.D., A.J.R.H., G.M.C.R.; Investigation: J.B.L.D., A.J.R.H., G.M.C.R.; Resources: A.J.R.H., G.M.C.R.; Data curation: J.B.L.D.; Writing - original draft: J.B.L.D.; Writing - review & editing: J.B.L.D., A.J.R.H., G.M.C.R.; Supervision: A.J.R.H., G.M.C.R.; Project administration: G.M.C.R.; Funding acquisition: A.J.R.H., G.M.C.R.

Funding

Epaulette sharks and chemicals were purchased personally by G.M.C.R. J.B.L.D., A.J.R.H. and G.M.C.R. were supported by the Marsden Fund of The Royal Society of New Zealand (14-UOA-210).

Data availability

The dataset supporting the result of this manuscript is available from the University of Auckland repository ResearchSpace: <https://auckland.figshare.com/s/0bbf1a73b9c7f62309bf>.

References

- Agutter, P. S. and Wheatley, D. N. (2004). Metabolic scaling: consensus or controversy? *Theor. Biol. Med. Model.* **1**, 13.
- Ali, S. S., Hsiao, M., Zhao, H. W., Dugan, L. L., Haddad, G. G. and Zhou, D. (2012). Hypoxia-adaptation involves mitochondrial metabolic depression and decreased ROS leakage. *PLoS ONE* **7**, e36801.
- Andrienko, T. N., Pasdois, P., Pereira, G. C., Owens, M. J. and Halestrap, A. P. (2017). The role of succinate and ROS in reperfusion injury - A critical appraisal. *J. Mol. Cell. Cardiol.* **110**, 1-14.
- Azzu, V., Parker, N. and Brand, M. D. (2008). High membrane potential promotes alkenal-induced mitochondrial uncoupling and influences adenine nucleotide translocase conformation. *Biochem. J.* **413**, 323-332.
- Bennett, M. B., Kyne, P. M. and Heupel, M. R. (2015). Hemiscyllum ocellatum. The IUCN Red List of Threatened Species 2015, e.T41818A68625284.
- Benzi, G., Arrigoni, E., Marzatico, F. and Villa, R. F. (1979). Influence of some biological pyrimidines on the succinate cycle during and after cerebral ischemia. *Biochem. Pharmacol.* **28**, 2545-2550.

- Benzi, G., Pastoris, O. and Dossena, M.** (1982). Relationships between gamma-aminobutyrate and succinate cycles during and after cerebral ischemia. *J. Neurosci. Res.* **7**, 193-201.
- Boutillier, R. G.** (2001). Mechanisms of cell survival in hypoxia and hypothermia. *J. Exp. Biol.* **204**, 3171-3181.
- Brand, M. D., Pakay, J. L., Ocloo, A., Kokoszka, J., Wallace, D. C., Brookes, P. S. and Cornwall, E. J.** (2005). The basal proton conductance of mitochondria depends on adenine nucleotide translocase content. *Biochem. J.* **392**, 353-362.
- Brookes, P. S.** (2005). Mitochondrial H(+) leak and ROS generation: an odd couple. *Free Radic. Biol. Med.* **38**, 12-23.
- Brown, G. C.** (1995). Nitric oxide regulates mitochondrial respiration and cell functions by inhibiting cytochrome oxidase. *FEBS Lett.* **369**, 136-139.
- Brown, J. C. L., Chung, D. J., Belgrave, K. R. and Staples, J. F.** (2012). Mitochondrial metabolic suppression and reactive oxygen species production in liver and skeletal muscle of hibernating thirteen-lined ground squirrels. *Am. J. Physiol. Regul. Integr. Comp. Physiol.* **302**, R15-R28.
- Brown, J. C. L., Chung, D. J., Cooper, A. N. and Staples, J. F.** (2013). Regulation of succinate-fuelled mitochondrial respiration in liver and skeletal muscle of hibernating thirteen-lined ground squirrels. *J. Exp. Biol.* **216**, 1736-1743.
- Cervós-Navarro, J. and Diemer, N. H.** (1991). Selective vulnerability in brain hypoxia. *Crit. Rev. Neurobiol.* **6**, 149-182.
- Chapman, C. A. and Renshaw, G. M. C.** (2009). Hematological responses of the grey carpet shark (*Chiloscyllium punctatum*) and the epaulette shark (*Hemiscyllium ocellatum*) to anoxia and re-oxygenation. *J. Exp. Zool. A Ecol. Genet. Physiol.* **311**, 422-438.
- Chapman, L. J., Chapman, C. A., Nordlie, F. G. and Rosenberger, A. E.** (2002). Physiological refugia: swamps, hypoxia tolerance and maintenance of fish diversity in the Lake Victoria region. *Comp. Biochem. Physiol. A Mol. Integr. Physiol.* **133**, 421-437.
- Chapman, C. A., Harahush, B. K. and Renshaw, G. M. C.** (2011). The physiological tolerance of the grey carpet shark (*Chiloscyllium punctatum*) and the epaulette shark (*Hemiscyllium ocellatum*) to anoxic exposure at three seasonal temperatures. *Fish Physiol. Biochem.* **37**, 387-399.
- Chen, Q., Camara, A. K. S., Stowe, D. F., Hoppel, C. L. and Lesnefsky, E. J.** (2007). Modulation of electron transport protects cardiac mitochondria and decreases myocardial injury during ischemia and reperfusion. *Am. J. Physiol. Cell Physiol.* **292**, C137-C147.
- Chinopoulos, C., Kiss, G., Kawamata, H. and Starkov, A. A.** (2014). Measurement of ADP-ATP exchange in relation to mitochondrial transmembrane potential and oxygen consumption. *Methods Enzymol.* **542**, 333-348.
- Chouchani, E. T., Pell, V. R., Gaude, E., Aksentijevic, D., Sundier, S. Y., Robb, E. L., Logan, A., Nadtochiy, S. M., Ord, E. N. J., Smith, A. C. et al.** (2014). Ischaemic accumulation of succinate controls reperfusion injury through mitochondrial ROS. *Nature* **515**, 431-435.
- Cooper, C. E. and Brown, G. C.** (2008). The inhibition of mitochondrial cytochrome oxidase by the gases carbon monoxide, nitric oxide, hydrogen cyanide and hydrogen sulfide: chemical mechanism and physiological significance. *J. Bioenerg. Biomembr.* **40**, 533-539.
- De Groot, H. and Rauen, U.** (2007). Ischemia-reperfusion injury: processes in pathogenetic networks: a review. *Transplant. Proc.* **39**, 481-484.
- Divakaruni, A. S. and Brand, M. D.** (2011). The regulation and physiology of mitochondrial proton leak. *Physiology (Bethesda)* **26**, 192-205.
- Dowd, W. W., Renshaw, G. M. C., Cech, J. J., Jr. and Kultz, D.** (2010). Compensatory proteome adjustments imply tissue-specific structural and metabolic reorganization following episodic hypoxia or anoxia in the epaulette shark (*Hemiscyllium ocellatum*). *Physiol. Genomics* **42**, 93-114.
- Dudgeon, C. L., Bennett, M. B. and Kyne, P. M.** (2016). *Chiloscyllium punctatum*. The IUCN Red List of Threatened Species 2016: e.T41872A68616745.
- Folbergrová, J., Ljunggren, B., Norberg, K. and Siesjö, B. K.** (1974). Influence of complete ischemia on glycolytic metabolites, citric acid cycle intermediates, and associated amino acids in the rat cerebral cortex. *Brain Res.* **80**, 265-279.
- Giusti, S., Converso, D. P., Poderoso, J. J. and Fiszer de Plazas, S.** (2008). Hypoxia induces complex I inhibition and ultrastructural damage by increasing mitochondrial nitric oxide in developing CNS. *Eur. J. Neurosci.* **27**, 123-131.
- Gnaiger, E.** (2014). *Mitochondrial Pathways and Respiratory Control: An Introduction to OXPHOS Analysis*, Vol. 1. OROBOROS MiPNet Publications.
- Hardy, D. L., Clark, J. B., Darley-Usmar, V. M. and Smith, D. R.** (1990). Reoxygenation of the hypoxic myocardium causes a mitochondrial complex I defect. *Biochem. Soc. Trans.* **18**, 549.
- Harris, E. J. and Manger, J. R.** (1969). Intersubstrate competitions and evidence for compartmentation in mitochondria. *Biochem. J.* **113**, 617-628.
- Hickey, A. J. R., Renshaw, G. M. C., Speers-Roesch, B., Richards, J. G., Wang, Y., Farrell, A. P. and Brauner, C. J.** (2012). A radical approach to beating hypoxia: depressed free radical release from heart fibres of the hypoxia-tolerant epaulette shark (*Hemiscyllium ocellatum*). *J. Comp. Physiol. B* **182**, 91-100.
- Javadov, S.** (2015). The calcium-ROS-pH triangle and mitochondrial permeability transition: challenges to mimic cardiac ischemia-reperfusion. *Front. Physiol.* **6**, 83.
- Kalogeris, T., Baines, C. P., Krenz, M. and Korthuis, R. J.** (2012). Cell biology of ischemia/reperfusion injury. *Int. Rev. Cell Mol. Biol.* **298**, 229-317.
- Kinnally, K. W., Peixoto, P. M., Ryu, S.-Y. and Dejean, L. M.** (2011). Is mPTP the gatekeeper for necrosis, apoptosis, or both? *Biochim. Biophys. Acta* **1813**, 616-622.
- Klingenberg, M.** (2008). The ADP and ATP transport in mitochondria and its carrier. *Biochim. Biophys. Acta* **1778**, 1978-2021.
- Klumpe, L., Savvatis, K., Westermann, D., Tschöpe, C., Rauch, U., Landmesser, U., Schultheiss, H.-P. and Dörner, A.** (2016). Transgenic overexpression of adenine nucleotide translocase 1 protects ischemic hearts against oxidative stress. *J. Mol. Med. (Berl.)* **94**, 645-653.
- Kondrashova, M., Zakharchenko, M. and Khunderyakova, N.** (2009). Preservation of the in vivo state of mitochondrial network for ex vivo physiological study of mitochondria. *Int. J. Biochem. Cell Biol.* **41**, 2036-2050.
- Last, P. R.** (2009). *Sharks and Rays of Australia*. Collingwood, VIC: CSIRO Publishing.
- Lutz, P. L. and Nilsson, G. E.** (1997). Contrasting strategies for anoxic brain survival—glycolysis up or down. *J. Exp. Biol.* **200**, 411-419.
- McLennan, H. R. and Degli Esposti, M.** (2000). The contribution of mitochondrial respiratory complexes to the production of reactive oxygen species. *J. Bioenerg. Biomembr.* **32**, 153-162.
- Mulvey, J. M. and Renshaw, G. M. C.** (2000). Neuronal oxidative hypometabolism in the brainstem of the epaulette shark (*Hemiscyllium ocellatum*) in response to hypoxic pre-conditioning. *Neurosci. Lett.* **290**, 1-4.
- Murphy, M. P.** (2009). How mitochondria produce reactive oxygen species. *Biochem. J.* **417**, 1-13.
- Murphy, M. P.** (2016). Understanding and preventing mitochondrial oxidative damage. *Biochem. Soc. Trans.* **44**, 1219-1226.
- Musatov, A. and Robinson, N. C.** (2012). Susceptibility of mitochondrial electron-transport complexes to oxidative damage. Focus on cytochrome c oxidase. *Free Radic. Res.* **46**, 1313-1326.
- Navet, R., Mouihys-Mickalad, A., Douette, P., Sluse-Goffart, C. M., Jarmuszkiewicz, W. and Sluse, F. E.** (2006). Proton leak induced by reactive oxygen species produced during in vitro anoxia/reoxygenation in rat skeletal muscle mitochondria. *J. Bioenerg. Biomembr.* **38**, 23-32.
- Nilsson, G. E. and Ostlund-Nilsson, S.** (2004). Hypoxia in paradise: widespread hypoxia tolerance in coral reef fishes. *Proc. Biol. Sci.* **271** Suppl. 3, S30-S33.
- Nilsson, G. E. and Renshaw, G. M.** (2004). Hypoxic survival strategies in two fishes: extreme anoxia tolerance in the North European crucian carp and natural hypoxic pre-conditioning in a coral-reef shark. *J. Exp. Biol.* **207**, 3131-3139.
- Paradies, G., Petrosillo, G., Pistolese, M. and Ruggiero, F. M.** (2002). Reactive oxygen species affect mitochondrial electron transport complex I activity through oxidative cardiolipin damage. *Gene* **286**, 135-141.
- Paradies, G., Petrosillo, G., Pistolese, M., Di Venosa, N., Federici, A. and Ruggiero, F. M.** (2004). Decrease in mitochondrial complex I activity in ischemic/reperfused rat heart: involvement of reactive oxygen species and cardiolipin. *Circ. Res.* **94**, 53-59.
- Pfleger, J., He, M. and Abdellatif, M.** (2015). Mitochondrial complex II is a source of the reserve respiratory capacity that is regulated by metabolic sensors and promotes cell survival. *Cell Death Dis.* **6**, e1835.
- Potts, D. C. and Swart, P. K.** (1984). Water temperature as an indicator of environmental variability on a coral reef. *Limnol. Oceanogr.* **29**, 504-516.
- Quinlan, C. L., Orr, A. L., Perevoshchikova, I. V., Treberg, J. R., Ackrell, B. A. and Brand, M. D.** (2012). Mitochondrial complex II can generate reactive oxygen species at high rates in both the forward and reverse reactions. *J. Biol. Chem.* **287**, 27255-27264.
- Renshaw, G. M. C. and Dyson, S. E.** (1999). Increased nitric oxide synthase in the vasculature of the epaulette shark brain following hypoxia. *Neuroreport* **10**, 1707-1712.
- Renshaw, G. M. C., Kerrisk, C. B. and Nilsson, G. E.** (2002). The role of adenosine in the anoxic survival of the epaulette shark, *Hemiscyllium ocellatum*. *Comp. Biochem. Physiol. B Biochem. Mol. Biol.* **131**, 133-141.
- Renshaw, G. M. C., Kutek, A. K., Grant, G. D. and Anoopkumar-Dukie, S.** (2012). Forecasting elasmobranch survival following exposure to severe stressors. *Comp. Biochem. Physiol. A Mol. Integr. Physiol.* **162**, 101-112.
- Richards, J. G., Wang, Y. S., Brauner, C. J., Gonzalez, R. J., Patrick, M. L., Schulte, P. M., Choppari-Gomes, A. R., Almeida-Val, V. M. and Val, A. L.** (2007). Metabolic and ionoregulatory responses of the Amazonian cichlid, *Astronotus ocellatus*, to severe hypoxia. *J. Comp. Physiol. B* **177**, 361-374.
- Rolfe, D. F. S. and Brand, M. D.** (1997). The physiological significance of mitochondrial proton leak in animal cells and tissues. *Biosci. Rep.* **17**, 9-16.
- Rouslin, W.** (1983). Mitochondrial complexes I, II, III, IV, and V in myocardial ischemia and autolysis. *Am. J. Physiol.* **244**, H743-H748.
- Routley, M. H., Nilsson, G. E. and Renshaw, G. M. C.** (2002). Exposure to hypoxia primes the respiratory and metabolic responses of the epaulette shark to progressive hypoxia. *Comp. Biochem. Physiol. A Mol. Integr. Physiol.* **131**, 313-321.
- Rubinsky, B.** (2003). Principles of low temperature cell preservation. *Heart Fail. Rev.* **8**, 277-284.
- Rytkönen, K. T., Renshaw, G. M. C., Vainio, P. P., Ashton, K. J., Williams-Pritchard, G., Leder, E. H. and Nikinmaa, M.** (2012). Transcriptional responses

- to hypoxia are enhanced by recurrent hypoxia (hypoxic preconditioning) in the epaulette shark. *Physiol. Genomics* **44**, 1090-1097.
- Starkov, A.** (2008). The role of mitochondria in reactive oxygen species metabolism and signalling. *Ann. N Y Acad. Sci.* **1147**, 37-52.
- Stensløkken, K.-O., Milton, S. L., Lutz, P. L., Sundin, L., Renshaw, G. M. C., Stecyk, J. A. W. and Nilsson, G. E.** (2008). Effect of anoxia on the electroretinogram of three anoxia-tolerant vertebrates. *Comp. Biochem. Physiol. A Mol. Integr. Physiol.* **150**, 395-403.
- Tretter, L., Patocs, A. and Chinopoulos, C.** (2016). Succinate, an intermediate in metabolism, signal transduction, ROS, hypoxia, and tumorigenesis. *Biochim. Biophys. Acta* **1857**, 1086-1101.
- Tuan, T.-C., Hsu, T.-G., Fong, M.-C., Hsu, C.-F., Tsai, K. K. C., Lee, C.-Y. and Kong, C.-W.** (2008). Deleterious effects of short-term, high-intensity exercise on immune function: evidence from leucocyte mitochondrial alterations and apoptosis. *Br. J. Sports Med.* **42**, 11-15.
- Val, A. L., Silva, M. N. P. and Almeida-Val, V. M. F.,** (1998). Hypoxia adaptation in fish of the Amazon: a never-ending task. *South Afr. J. Zool. Suid-Afrikaanse tydskrif vir dierkunde* **33**, 107-114.
- Val, A. L., Gomes, K. R. M. and de Almeida-Val, V. M. F.** (2015). Rapid regulation of blood parameters under acute hypoxia in the Amazonian fish *Prochilodus nigricans*. *Comp. Biochem. Physiol. A Mol. Integr. Physiol.* **184**, 125-131.
- Winter, J., Klumpe, I., Heger, J., Rauch, U., Schultheiss, H.-P., Landmesser, U. and Dörner, A.** (2016). Adenine nucleotide translocase 1 overexpression protects cardiomyocytes against hypoxia via increased ERK1/2 and AKT activation. *Cell. Signal.* **28**, 152-159.
- Wise, G., Mulvey, J. M. and Renshaw, G. M. C.** (1998). Hypoxia tolerance in the epaulette shark (*Hemiscyllium ocellatum*). *J. Exp. Zool.* **281**, 1-5.
- Wojtovich, A. P. and Brookes, P. S.** (2008). The endogenous mitochondrial complex II inhibitor malonate regulates mitochondrial ATP-sensitive potassium channels: implications for ischemic preconditioning. *Biochim. Biophys. Acta* **1777**, 882-889.
- Zakharchenko, M. V., Zakharchenko, A. V., Khunderyakova, N. V., Tutukina, M. N., Simonova, M. A., Vasilieva, A. A., Romanova, O. I., Fedotcheva, N. I., Litvinova, E. G., Maevsky, E. I. et al.** (2013). Burst of succinate dehydrogenase and alpha-ketoglutarate dehydrogenase activity in concert with the expression of genes coding for respiratory chain proteins underlies short-term beneficial physiological stress in mitochondria. *Int. J. Biochem. Cell Biol.* **45**, 190-200.